Gradient of Rigidity in the Lamellipodia of Migrating Cells Revealed by Atomic Force Microscopy

Valérie M. Laurent,*† Sandor Kasas,‡§ Alexandre Yersin,‡ Tilman E. Schäffer,‖ Stefan Catsicas,‡ Giovanni Dietler,¶ Alexander B. Verkhovsky,* and Jean-Jacques Meister*

*Laboratory of Cell Biophysics, Ecole Polytechnique Fédérale, Lausanne, Switzerland; †Physopathologie et Thérapeutique Respiratoires, INSERM UMR492, Créteil, France; ‡Institut de Neurobiologie Cellulaire, Ecole Polytechnique Fédérale, Lausanne, Switzerland; §Département de Biologie Cellulaire et de Morphologie, University of Lausanne, Lausanne, Switzerland; ¶Institut de Physique de la Matière Complexe, Ecole Polytechnique Fédérale, Lausanne, Switzerland; and ‖Center for NanoTechnology (CeNTech) and Institute of Physics, University of Münster, Münster, Germany

ABSTRACT Changes in mechanical properties of the cytoplasm have been implicated in cell motility, but there is little information about these properties in specific regions of the cell at specific stages of the cell migration process. Fish epidermal keratocytes with their stable shape and steady motion represent an ideal system to elucidate temporal and spatial dynamics of the mechanical state of the cytoplasm. As the shape of the cell does not change during motion and actin network in the lamellipodia is nearly stationary with respect to the substrate, the spatial changes in the direction from the front to the rear of the cell reflect temporal changes in the actin network after its assembly at the leading edge. We have utilized atomic force microscopy to determine the rigidity of fish keratocyte lamellipodia as a function of time/distance from the leading edge. Although vertical thickness remained nearly constant throughout the lamellipodia, the rigidity exhibited a gradual but significant decrease from the front to the rear of the lamellipodia. The rigidity profile resembled closely the actin density profile, suggesting that the dynamics of rigidity are due to actin depolymerization. The decrease of rigidity may play a role in facilitating the contraction of the actin-myosin network at the lamellipodium/cell body transition zone.

INTRODUCTION

Cell motility is ultimately a mechanical phenomenon. Early theories of cell motility considered changes of the mechanical state of the cytoplasm, such as gel/sol transformations, an important part of the motility process. More recently, critical advances have been made in understanding the molecular events involved in cell migration, in particular, of the complex chain of biochemical reactions leading to the actin assembly at the leading edge of the cell (1–5). Actin assembly is believed to provide the force for protrusion and to generate the cytoskeletal structure that is sufficiently strong mechanically to transmit and withstand forces and at the same time sufficiently flexible to adapt to the changes of the cell shape and behavior. Characterization of the forces generated by migrating cells and of their mechanical properties represents a level of description that is complementary to the biochemical and structural data.

The forces at the cell-substrate interface have been measured using micromachined and elastic substrates (6,7), and the mechanical properties of the cells themselves were accessed by a variety of methods including micromanipulation with microneedles and plates, microrheology using embedded exogenous particles (3,8–10), and atomic force microscopy (AFM). AFM represents an attractive tool to investigate cellular mechanics since it allows for simultaneous evaluation of local mechanical properties and topography of the living cell in an aqueous environment with a spatial resolution up to a few nanometers and force sensitivity in the piconewton range (11).

Previous AFM studies were aimed to obtain high resolution topographic images of the cells and subcellular components, to reveal mechanical differences between different cellular domains, such as the peripheral and perinuclear cytoplasm, to elucidate mechanical contributions of different cytoskeletal structures, and also to draw functional correlation between the state of the cell and its mechanical properties (12–19).

In a few studies, the spatial and temporal dynamics of the mechanical properties of the cell edge in the process of spreading and motility were analyzed by AFM (20,21). This analysis may help to answer questions related to the mechanisms of cell protrusion and contraction. In particular, the notion that the actin assembly provides the protrusive force is consistent with a rigid actin network at the leading edge (2,5,22–24). However, some types of cells form bleblike protrusions at the leading edge containing few actin filaments (25,26). These observations are consistent with the models suggesting that protrusion may be driven by forces other than actin polymerization, e.g., osmotic or hydrostatic forces, whereas the actin network may fill the space subsequently to protrusion. The mechanism driven by osmotic or hydrostatic pressure would imply that the leading edge is mechanically weak with respect to the other parts of the cell. On the other hand, it has been suggested that the

Submitted September 8, 2004, and accepted for publication February 23, 2005.

Address reprint requests to Valérie M. Laurent, Laboratoire de Neuro-Physique Cellulaire, EA3817 Université René Descartes, 45 rue des Saints-Pères, 75270 Paris Cedex 06, France. Tel.: 33-1-42-86-20-46; Fax: 33-1-42-86-20-85; E-mail: valerie.laurent@univ-paris5.fr.

0006-3495/05/07/667/09 $2.00

doi: 10.1529/biophysj.104.052316

solation of cytoplasmic actin gel may be a prerequisite to contraction by myosin motors (27). The measurement of the dynamics of mechanical properties associated with the events of protrusion and contraction is therefore necessary to validate these and other models. However, the irregularity of the edge behavior of cells such as fibroblasts, exhibiting alternating phases of protrusion, withdrawal, and ruffling may complicate the analysis and limit the conclusions. To overcome these shortcomings, it is beneficial to use a model cell with regular motile behavior. Fish epidermal keratocytes with their well-defined leading lamellipodia, stable shape, and fast and persistent motion represent an ideal system to examine the mechanics of the leading edge (28,29).

A freely locomoting keratocyte cell consists of two major domains, a wide and flat leading lamellipodium filled with a dense actin network and the trailing cell body containing the nucleus and other organelles. The actin network assembled at the leading edge of the lamellipodium does not move forward with respect to the substratum as the leading edge advances (30,31). Therefore, the distance from the leading edge reflects the time after the initial network assembly, and the temporal dynamics of the network properties become recorded in space. Since the actin density decreases with the distance from the leading edge due to depolymerization, it has been suggested that the rigidity of the lamellipodia also decreases and that this facilitates contraction of the actin/myosin II network at the lamellipodium/cell body boundary (29,32). Contraction has been implicated in the forward translocation of the cell body; however, the spatial and temporal dynamics of the rigidity of keratocyte lamellipodia have not been investigated.

Here we examine the properties of the keratocyte lamellipodia using AFM, with emphasis on the detection of possible variations of the mechanical properties with the distance from the edge.

MATERIALS AND METHODS

Keratocyte culture

Keratocyte culture was carried out essentially as described by Svitkina et al. (29). Briefly, black tetra keratocytes were cultured in DMEM (Hepes modification; Sigma Chemical, St. Louis, MO) supplemented with 10% FBS and antibiotics. Fish scales were extracted with tweezers, placed on the surface of a dry 50-mm petri dish, and allowed to adhere for 30–60 s to prevent floating. Culture medium was then added and the scales were kept at 30°C overnight to allow for migration of keratocytes from the scale onto the dish. Colonies of migrated cells were treated with 0.2% trypsin and 0.02% EDTA in phosphate-buffered saline (PBS) for ~30–60 s and the cells were allowed to recover for 1–3 h before AFM experiments in 3 ml of fresh culture medium containing 30% purified water, because it was observed that keratocytes in the diluted medium exhibit a more regular shape and motile behavior than in a complete medium.

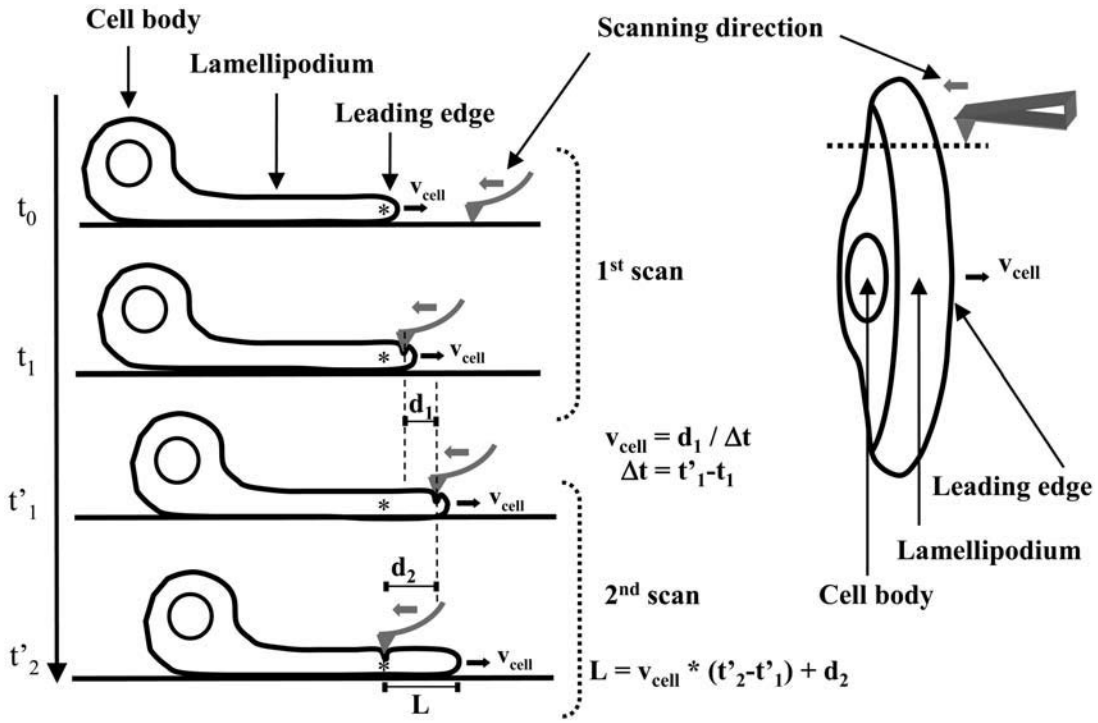

FIGURE 1 A schematic illustration of AFM measurements on migrating fish keratocyte. (*Left*) Side view of moving cell. (*Right*) Top view. The black and shaded arrows indicate the direction of the migrating keratocyte and the AFM tip, respectively. Average speed of cell migration, v_{cell}, is calculated as the difference, d_1, between the leading edge positions in two subsequent scans divided by the time interval, $t'_1 - t_1$, between the scans. At time t_2, the distance L from the leading edge is deduced from the average speed v_{cell} and the difference, d_2, between the tip positions at time t_2 and at time t'_1 of the leading-edge measurement. The asterisk indicates the fixed position with respect to the substratum.

Rhodamine-phalloidin staining and fluorescence images

Fish keratocytes were stained for F-actin with rhodamine-phalloidin after glutaraldehyde fixation as described previously (29,33) but the fixation procedure was modified to minimize the time between AFM measurements and immobilization of the cells. A few seconds after the AFM measurement, culture medium in the dish was replaced with a 2% glutaraldehyde solution in culture medium. After 10 min of incubation, fixed cells were rinsed twice with PBS, permeabilized in 1% Triton X-100 in PBS, treated with 2 mg/ml sodium borohydride in PBS (two treatments of 5 min each), and stained with rhodamine-phalloidin to reveal F-actin. Fluorescence images of fixed cells were taken using Nikon Eclipse T300 inverted microscope and Micromax PB1300 cooled CDD camera (Roper Scientific, Tucson, AZ) operated with Metamorph imaging software (Universal Imaging, Union City, CA).

Atomic force microscopy

We used a combination of commercial AFM (Bioscope, Digital Instruments, Santa Barbara, CA) with an inverted microscope for the positioning of the AFM tip on the course of migrating keratocytes with micrometer precision. Commercially available silicon-nitride cantilevers with low force constant of typically 0.06 N/m (Veeco Instruments, Woodbury, NY) were employed. Both elastic properties and height profiles of keratocytes were measured using the force-volume mode of the AFM. In this mode, position and deflexion of the AFM cantilever are continuously recorded as it approaches the sample surface until it reaches a user-defined deflexion. Then the cantilever is lifted and moved to the following positions over the surface of the sample. The mode basically consists of recording hundreds of force-distance curves (cantilever deflexion versus sample z-position) all over the sample.

We focused on the measurements of the elastic modulus and height profiles of keratocyte lamellipodia in the direction along the axis of cell locomotion (perpendicular to the leading edge). For this purpose, the AFM was operated in a one-dimensional scanning mode. More specifically, the tip spanned a distance of 4.5 μm along a single line in the direction opposite to cell locomotion, and the force/indentation curves were recorded at 16 points along this interval at a frequency of 4 Hz. After completion of the scan the tip returned to the initial position, and the sequence was repeated. Since one scan interval is only ~½ of the lamellipodium size (~10 μm from front to back), several scans were performed on the lamellipodium of the same cell while it was moving through the area, until the whole span of the lamellipodium was covered. The first scans started at the substrate in front of the moving cell and the last ended over the cell body. The measurements of the lamellipodia height and elastic modulus at different locations were then represented as a function of the distance from the leading edge. To determine this distance, the position of the leading edge at every time point was estimated based on the average speed of cell migration, which was calculated as the difference between the leading edge positions in the two subsequent scans divided by the time interval between the scans (Fig. 1). Typically, the cells moved at ~0.2 μm/s, and the distance between the two subsequent scan points in the substrate coordinates was 0.3 μm, which means that the difference between the scan points in terms of distance from the leading edge was 0.35 μm. This procedure allowed recording multiple force curves at different distances from the leading edge and at different time points so that both spatial and temporal variability of the edge properties could be evaluated.

Determination of the real height (H) and the elastic modulus (E) of the lamellipodium

True height, H, and elastic modulus, E, were determined from force curves. Theoretically, force curves should show that the measured cantilever deflexion is zero as long as the AFM tip is off the sample and increases beyond the contact point with the sample. Nevertheless, experimental force curves often display some repulsive forces in the vicinity of the cell, e.g., curves exhibit a linear and slow cantilever deflexion increase before coming in contact with

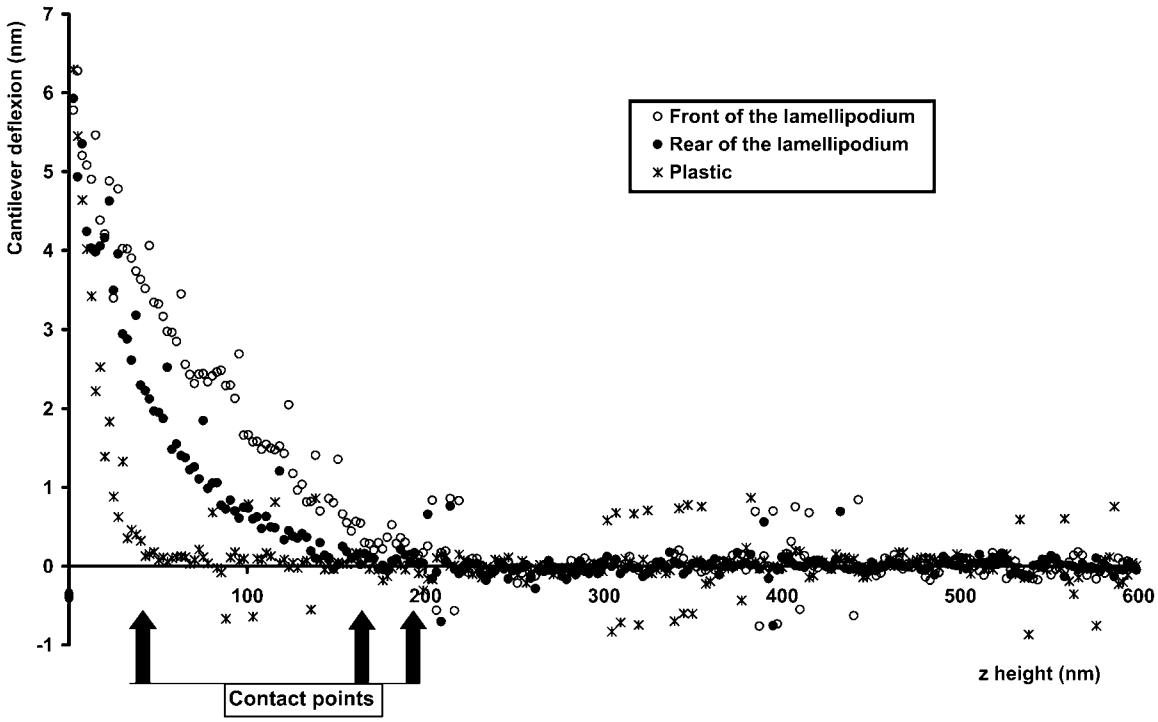

FIGURE 2 Typical force curves obtained for two different locations on a migrating keratocyte lamellipodium and for one location on the plastic cellular dish. The different z-height values for which the tip comes into contact with the lamellipodium surface or the plastic cellular dish are indicated by black arrows. True height values of lamellipodium were calculated from the difference between the contact point heights of the lamellipodium and the plastic dish.

the sample. Experimental force curves for the migrating keratocyte lamellipodium and for the plastic cellular dish are shown in Fig. 2. The repulsive force effects have been subtracted from these curves. The different z-height values for which the tip comes into contact with the lamellipodium or the plastic dish are indicated on this figure. These z-height values of contact were estimated by a linear regression fit of the right part of the curve (where the tip is off the sample) and determining where the cantilever deflexion increases nonlinearly with the tip displacement. The true height values H of lamellipodium were calculated from the difference in z-height values of contact with the lamellipodium and the z-height value of contact with the plastic dish. The experimental data point measured on the plastic dish just before encountering the leading edge of the migrating cells was used for this calculation.

The determination of the elastic modulus from the force curves was performed using Sneddon's modification of the Hertz model for a purely elastic indentation in a flat and soft sample by a stiff cone (20,34–36). The model predicts a relationship between the applied loading force F and the indentation depth δ of the AFM cantilever into the soft sample:

$$F = 2/\pi \times \tan\alpha \times E/(1-\nu^2) \times \delta^2, \qquad (1)$$

where ν is Poisson's ratio of the sample and α is the half-opening angle of the AFM tip. Poisson's ratio was assumed to be 0.5 because the cell was considered incompressible. The applied loading force was calculated from the measured cantilever deflexion $d(z)$ and the force constant k of the cantilever as follows: $F = k \times d(z)$. The indentation depth in the cell was calculated from the cantilever deflexion and the z-height as follows: $\delta = z - d(z)$. The elastic modulus values were determined from the transformation of experimental force curves into force-square indentation curves and the linear regression fit by the Hertz model equation (Eq. 1) according to Radmacher et al. (35).

To minimize the influence of the underlying substrate, only the experimental data points obtained for indentation depth <70 nm were used to fit with the Hertz model equation. However, even this small indentation depth is significant with respect to the thickness of keratocyte lamellipodia (150–200 nm). Consequently, we could not exclude that the elastic modulus was overestimated due to the substrate influence. The values of the elastic modulus obtained using Hertz model should thus be considered as an apparent elastic modulus or an upper limit for the true elastic modulus of the cell. Differences in the apparent elastic modulus between different regions of the cell are nevertheless expected to reflect the differences in the true elastic modulus, provided that the cell thickness does not change significantly.

In all these experiments, we considered the extension path of the force-distance curves for the determination of the elastic modulus. This choice was motivated by the concern that the actin filaments that may have been displaced by the AFM tip during the extension path could not participate any more in the elastic response of the cell during the retraction part of the curves. Nevertheless, elastic modulus values calculated on the extension segment were similar to those calculated on the retraction segment of the force-distance curves for the different locations on the lamellipodium. Consecutive scans over the same area did not show any significant difference in the topographic and elastic properties of the lamellipodium, suggesting that permanent deformations and their influence on the measurements could be neglected.

In our measurements, the indentation speed of the tip was in the order of 0.25 μm/s. This relatively high speed was necessary to effectively scan the lamellipodia of rapidly migrating keratocytes (cell migration velocity, 0.25 μm/s). A previous study of three different cell types demonstrated that the relative contribution of viscous losses to the elastic modulus is either negligible or not significant for this order of tip velocity (16), suggesting that viscous losses could also be neglected in our experiments.

RESULTS

The AFM procedure does not disrupt the motility and cytoskeletal organization of keratocytes

During the AFM experiment, keratocytes continued to migrate normally, and no significant changes in their shape or behavior were observed. To test whether the organization of actin in the keratocyte lamellipodium is affected by the AFM measurements, the cells were fixed and stained for F-actin immediately after the experiment (Fig. 3). The staining revealed typical F-actin organization and distribution with a characteristic decrease of actin density from the front to the rear of the lamellipodium (29,32). For the cell shown in Fig. 3, the ratio of actin density at the front of the lamellipodium to that at its back was 1.53, which is similar to

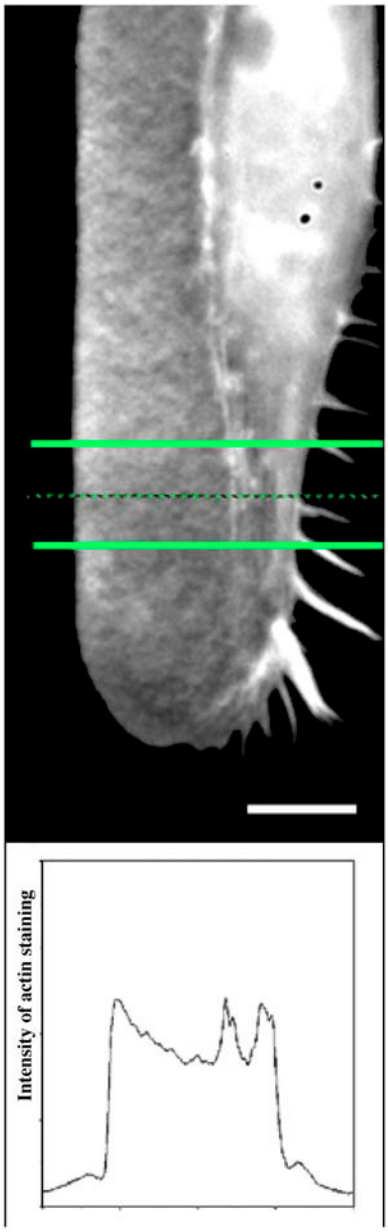

FIGURE 3 F-actin organization observed by fluorescence microscopy in a keratocyte measured by the AFM technique. Actin distribution is revealed by rhodamine-phalloidin. The actin intensity profile within the cell area indicated in the image is shown in the inset and this illustrated the actin gradient in the lamellipodium. Scale bar, 5 μm.

previously reported values (29). Thus, in addition to the behavior and shape of keratocyte lamellipodium, the actin distribution also was apparently unaffected by the AFM measurements.

Elastic properties of keratocyte lamellipodium

We focused on the measurement of the elastic properties of keratocyte lamellipodia depending on the distance from the leading edge (see Materials and Methods). Typical force-indentation curves obtained on the keratocyte lamellipodia are shown in Fig. 4. Two locations of the same lamellipodium are illustrated, one close to the leading edge of the cell and the other at the back of the lamellipodium, next to the cell body. Comparison of the curves shows that the same cantilever deflexion (force) corresponded to a smaller indentation at the front of the lamellipodium than at its back, indicating that the front part of the lamellipodium was stiffer. Consistent with this observation, the Hertz model fit produced a higher apparent elastic modulus value for the front of the lamellipodium.

To evaluate the variation in the apparent elastic modulus of the lamellipodia in a systematic way, the values obtained for different locations were plotted as a function of the distance from the leading edge. Fig. 5 shows the combined data from three representative cells, which demonstrate that the values of the elastic modulus exhibited a tendency to decrease from ~55 kPa at the front of the lamellipodium to ~10 kPa at its rear. This trend was apparent despite irregular

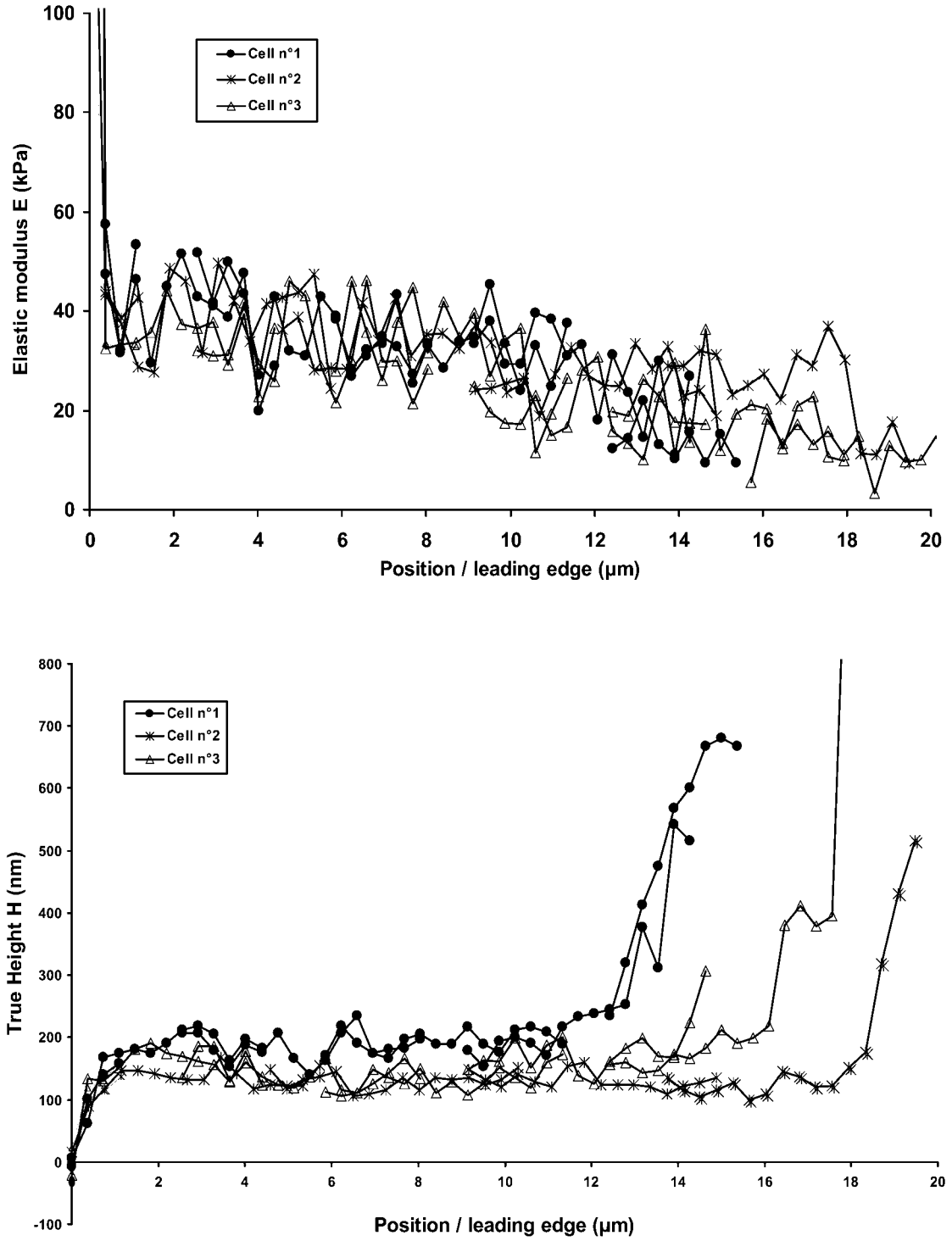

FIGURE 5 Elastic modulus and height profiles of lamellipodia for three different migrating keratocytes. Lamellipodia lengths are ~12 μm (●), 15 μm (△), and 17 μm (*). The elastic modulus, E, decreases from ~55 kPa on the leading edge down to ~10 kPa on the rear edge, whereas the true height, H, is approximately constant. This indicates that keratocyte lamellipodium is more rigid at the leading edge than at the rear part.

DISCUSSION

In this report, we use AFM to characterize the rigidity profile of a well-defined protrusive organelle, the lamellipodium, of a persistently moving cell, fish epidermal keratocyte. The mechanical properties of the active edge of migrating cells have been long a subject of discussion and some controversy (see Introduction for references). The idea of actin polymerization providing the protrusive force is consistent with a rigid leading

TABLE 1 Quantification of the elastic modulus reduction in the lamellipodia for nine different migrating keratocytes

Cell number	Elastic modulus at leading edge E (kPa)	Elastic modulus decrease by length unit (kPa/μm)	Length of lamellipodium (μm)	Total elastic modulus reduction ΔE (kPa)	Relative elastic modulus reduction $\Delta E/E$
1	26	−0.2	9.4	−2.2	−0.1
2	30	−2.1	7.4	−15.9	−0.5
3	44	−4.8	8.3	−39.9	−0.9
4	26	−1.7	8.0	−13.7	−0.5
5	34	−1.3	8.1	−10.8	−0.3
6	21	−0.6	9.7	−6.1	−0.3
7	41	−1.0	17.2	−16.7	−0.4
8	44	−1.3	12.1	−15.3	−0.3
9	39	−1.3	15.7	−21.2	−0.5
Mean	34	−1.6	10.7	−15.7	−0.4
Standard deviation	8	1.3	3.6	10.7	0.2

edge of the cell, whereas some other theories suggested that the protrusive activity is associated with mechanical weakening of the edge. Although the overwhelming amount of structural and biochemical evidence supports polymerization-driven protrusion, previous AFM measurements did register the reduction of the rigidity at the protruding edge of the cell (21).

We have estimated the elastic modulus of the front edge of the keratocyte lamellipodium at 10–55 kPa. It is necessary to note that these values represent only apparent stiffness, because the lamellipodium is very thin (140–200 nm) and the indentation by the AFM probe in our experiments was significant with respect to thickness of the lamellipodia. When the indentation of the sample in the process of measurement is significant with respect to its thickness, the rigidity may be overestimated due to the influence of the stiff underlying substrate. However, for an object of uniform thickness, the obtained values of apparent stiffness truthfully represent the differences in the true stiffness. The values we obtained for the elastic modulus of the keratocyte leading edge were several times higher than the values measured by AFM at the active edges of a few other cell types (20,21). It is unlikely that our estimation differs from other reports due to the substrate effect. The values of the elastic modulus in our study were determined using an even lower range of loading forces than previously employed (up to 100 pN as compared to 100–320 pN (20,21)), and therefore the substrate effect is unlikely to be more significant than in the other studies. Consequently, the differences in rigidity may reflect the differences in the structure of the leading edge between different types of cells.

The cells of fibroblastic and epithelial origin that were previously studied by AFM usually exhibit a small and rather flexible lamellipodium. It often represents a narrow (from ~1- to 2-μm-wide) band at the cell periphery, which forms transiently in the motility cycle and is closely followed by a different cell domain, the lamella. The lamella is characterized by a sparser actin network than in the lamellipodia and by the presence of contractile actomyosin bundles and microtubules. Without the knowledge of the exact actin organization at the time and the site of the AFM measurement, it is difficult to correlate the mechanical properties of the active edge to the cytoskeletal organization of the lamellipodia or that of the lamella. This could be a reason for the apparent variability in the mechanical properties.

In contrast to many other cell types, keratocytes move persistently, with a stable and large lamellipodium that typically measures ~10 μm from front to back. Therefore, the keratocyte model seems ideal to correlate the cytoskeletal organization at the cell edge with the mechanical properties. The high rigidity of keratocyte lamellipodia in comparison to those of other cells may reflect relative density of the lamellipodial actin network. Our AFM results are thus consistent with the ultrastructural studies that demonstrated extremely high density of the actin network in the keratocyte lamellipodia (23,29). Importantly, we also find that the rigidity is highest at the front protruding edge of the lamellipodia and gradually decreases with the distance from the edge, whereas the vertical thickness of the lamellipodia remains nearly constant. Note that even if the measurement of the absolute rigidity value is influenced by a stiff underlying substrate, the finding of the gradient of rigidity within the cell is independent of the substrate influence, since the thickness of the lamellipodia is constant and the mechanical properties of the substrate are homogeneous. This gradient of rigidity from the front to the back of lamellipodia mimics closely the gradient of actin density in keratocyte lamellipodia, which was established in several previous studies (29,37) and confirmed in this study (Fig. 3). Thus, not only is the measured high rigidity of keratocyte lamellipodia consistent with the overall high density of actin network in these cells, but the rigidity is also spatially correlated to the actin density within each individual cell. These findings are at variance with the report of Rotsch et al. (21), where the thickness of the cell edge was found to increase and the rigidity to decrease during protrusion. However, in the study of Rotsch et al., the rigidity was not compared to the dynamics of actin density. Thus, it is unclear whether the actin density in the cells studied by Rotsch et al. (21) also decreased during protrusion, or the decrease of rigidity was independent of the dynamics of actin density. Our findings are consistent with the

rigid actin network at the leading edge pushing the membrane forward in the process of protrusion. In contrast, the hypotheses postulating solation of the cytoplasm as a prerequisite for protrusion are not supported by these findings.

The finding of the gradient of rigidity in the lamellipodia is significant not only in relation to the protrusion mechanism, but also with respect to the mechanism of the cell-body translocation. It has been long speculated that the solation of cytoplasmic actin gel precedes and facilitates its contraction mediated by myosin motors (27). One of the models of the mechanism of keratocyte translocation, the dynamic network contraction hypothesis, suggests that the forward motion of the cell body is driven by the contraction of an actin-myosin network at the transition zone between the lamellipodium and the cell body (29,32). To ensure the persistent motion of the cell, it is essential that the contraction is limited to this zone and does not extend to the front of the lamellipodium. The gradient of rigidity in the lamellipodium may be an important factor facilitating the contraction at the specific site (the back of the lamellipodium where the rigidity is the lowest), and precluding the contraction at other sites. Thus, the gradient of rigidity may be a part of the cell polarization mechanism necessary to establish and maintain the direction of cell migration.

In summary, we have investigated mechanical properties of a well-defined and stable protrusive organelle of the cell, the lamellipodium of migrating fish epidermal keratocytes. We found a gradient of rigidity in the lamellipodium, which has important implications both for protrusion and contraction mechanisms. Our study represents a step toward generating a detailed map of mechanical properties correlated to the cytoskeletal organization and to the migratory state of the cell, which is necessary for the comprehensive understanding of the biophysics of cell motility.

This work was supported by Swiss Science Foundation grant 31-61589 (A.B.V.). V.M.L. was supported by a ''Bourse de formation à l'étranger 2001'' grant (BDF 01 Contrat No. 000006495) from the Institut National de la Santé et de la Recherche Médicale (INSERM). T.E.S. was supported by the Gemeinnützige Hertie-Stiftung/Stifterverband für die Deutsche Wissenschaft.

REFERENCES

1. Borisy, G. G., and T. M. Svitkina. 2000. Actin machinery: pushing the envelope. *Curr. Opin. Cell Biol.* 12:104–112.
2. Condeelis, J. 1993. Life at the leading edge: the formation of cell protrusions. *Annu. Rev. Cell Biol.* 9:411–444.
3. Lauffenburger, D. A., and A. F. Horwitz. 1996. Cell migration: a physically integrated molecular process. *Cell.* 84:359–369.
4. Mitchison, T. J., and L. P. Cramer. 1996. Actin-based cell motility and cell locomotion. *Cell.* 84:371–379.
5. Pollard, T. D., L. Blanchoin, and R. D. Mullins. 2000. Molecular mechanisms controlling actin filament dynamics in nonmuscle cells. *Annu. Rev. Biophys. Biomol. Struct.* 29:545–576.
6. Galbraith, C. G., and M. P. Sheetz. 1997. A micromachine device provides a new bend on fibroblast traction forces. *Proc. Natl. Acad. Sci. USA.* 94:9114–9118.
7. Dembo, M., and Y. L. Wang. 1999. Stresses at the cell-to-substrate interface during locomotion of fibroblasts. *Biophys. J.* 76:2307–2316.
8. Nagayama, M., H. Haga, and K. Kawabata. 2001. Drastic change of local stiffness distribution correlating to cell migration in living fibroblasts. *Cell Motil. Cytoskeleton.* 50:173–179.
9. Laurent, V. M., S. Henon, E. Planus, R. Fodil, M. Balland, D. Isabey, and F. Gallet. 2002. Assessment of mechanical properties of adherent living cells by bead micromanipulation: comparison of magnetic twisting cytometry vs optical tweezers. *J. Biomech. Eng.* 124: 408–421.
10. Tseng, Y., T. P. Kole, and D. Wirtz. 2002. Micromechanical mapping of live cells by multiple-particle-tracking microrheology. *Biophys. J.* 83:3162–3176.
11. Domke, J., S. Dannohl, W. J. Parak, O. Muller, W. K. Aicher, and M. Radmacher. 2000. Substrate dependent differences in morphology and elasticity of living osteoblasts investigated by atomic force microscopy. *Colloids Surf. B Biointerfaces.* 19:367–379.
12. Henderson, E., P. G. Haydon, and D. S. Sakaguchi. 1992. Actin filament dynamics in living glial cells imaged by atomic force microscopy. *Science.* 257:1944–1946.
13. Schneider, S. W., K. C. Sritharan, J. P. Geibel, H. Oberleithner, and B. P. Jena. 1997. Surface dynamics in living acinar cells imaged by atomic force microscopy: identification of plasma membrane structures involved in exocytosis. *Proc. Natl. Acad. Sci. USA.* 94: 316–321.
14. A-Hassan, E., W. F. Heinz, M. D. Antonik, N. P. D'Costa, S. Nageswaran, C. A. Schoenenberger, and J. H. Hoh. 1998. Relative microelastic mapping of living cells by atomic force microscopy. *Biophys. J.* 74:1564–1578.
15. Hoh, J. H., and C. A. Schoenenberger. 1994. Surface morphology and mechanical properties of MDCK monolayers by atomic force microscopy. *J. Cell Sci.* 107:1105–1114.
16. Mathur, A. B., A. M. Collinsworth, W. M. Reichert, W. E. Kraus, and G. A. Truskey. 2001. Endothelial, cardiac muscle and skeletal muscle exhibit different viscous and elastic properties as determined by atomic force microscopy. *J. Biomech.* 34:1545–1553.
17. Radmacher, M. 2002. Measuring the elastic properties of living cells by the atomic force microscope. *Methods Cell Biol.* 68:67–90.
18. Sato, M., K. Nagayama, N. Kataoka, M. Sasaki, and K. Hane. 2000. Local mechanical properties measured by atomic force microscopy for cultured bovine endothelial cells exposed to shear stress. *J. Biomech.* 33:127–135.
19. Tao, N. J., S. M. Lindsay, and S. Lees. 1992. Measuring the microelastic properties of biological material. *Biophys. J.* 63:1165–1169.
20. Rotsch, C., K. Jacobson, and M. Radmacher. 1999. Dimensional and mechanical dynamics of active and stable edges in motile fibroblasts investigated by using atomic force microscopy. *Proc. Natl. Acad. Sci. USA.* 96:921–926.
21. Rotsch, C., K. Jacobson, J. Condeelis, and M. Radmacher. 2001. EGF-stimulated lamellipod extension in adenocarcinoma cells. *Ultramicroscopy.* 86:97–106.
22. Mogilner, A., and G. Oster. 1996. Cell motility driven by actin polymerization. *Biophys. J.* 71:3030–3045.
23. Small, J. V., A. Rohlfs, and M. Herzog. 1993. Actin and cell movement. *Symp. Soc. Exp. Biol.* 47:57–71.
24. Pantaloni, D., C. Le Clainche, and M. F. Carlier. 2001. Mechanism of actin-based motility. *Science.* 292:1502–1506.
25. Keller, H. U. 2000. Redundancy of lamellipodia in locomoting Walker carcinosarcoma cells. *Cell Motil. Cytoskeleton.* 46:247–256.
26. Keller, H., A. D. Zadeh, and P. Eggli. 2002. Localised depletion of polymerised actin at the front of Walker carcinosarcoma cells increases the speed of locomotion. *Cell Motil. Cytoskeleton.* 53: 189–202.

27. Taylor, D. L., and M. Fechheimer. 1982. Cytoplasmic structure and contractility: the solation–contraction coupling hypothesis. *Philos. Trans. R. Soc. Lond. B Biol. Sci.* 299:185–197.

28. Lee, J., A. Ishihara, and K. Jacobson. 1993. The fish epidermal keratocyte as a model system for the study of cell locomotion. *Symp. Soc. Exp. Biol.* 47:73–89.

29. Svitkina, T. M., A. B. Verkhovsky, K. M. McQuade, and G. G. Borisy. 1997. Analysis of the actin-myosin II system in fish epidermal keratocytes: mechanism of cell body translocation. *J. Cell Biol.* 139:397–415.

30. Jurado, C., J. R. Haserick, and J. Lee. 2004. Slipping or gripping? Fluorescent speckle microscopy in fish keratocytes reveals two different mechanisms for generating a retrograde flow of actin. *Mol. Biol. Cell.* 16:507–518.

31. Vallotton, P., G. Danuser, S. Bohnet, J.-J. Meister, and A. B. Verkhovsky. Tracking retrograde flow in keratocytes: news from the front. *Mol. Biol. Cell.* 16:1223–1231.

32. Verkhovsky, A. B., T. M. Svitkina, and G. G. Borisy. 1999. Network contraction model for cell translocation and retrograde flow. *Biochem. Soc. Symposium.* 65:207–222.

33. Svitkina, T. M., and G. G. Borisy. 1998. Correlative light and electron microscopy of the cytoskeleton of cultured cells. *Methods Enzymol.* 298:570–592.

34. Mathur, A. B., G. A. Truskey, and W. M. Reichert. 2000. Atomic force and total internal reflection fluorescence microscopy for the study of force transmission in endothelial cells. *Biophys. J.* 78:1725–1735.

35. Radmacher, M., M. Fritz, C. M. Kacher, J. P. Cleveland, and P. K. Hansma. 1996. Measuring the viscoelastic properties of human platelets with the atomic force microscope. *Biophys. J.* 70:556–567.

36. Sneddon, I. N. 1965. *Int. J. Eng. Sci.* 3:47–57.

37. Small, J. V., M. Herzog, and K. Anderson. 1995. Actin filament organisation in the fish keratocyte lamellipodium. *J. Cell Biol.* 129:1275–1286.